

JoVALE: Detecting Human Actions in Video Using Audiovisual and Language Contexts

Taein Son^{1*}, Soo Won Seo^{2*}, Jisong Kim¹, Seok Hwan Lee¹, Jun Won Choi^{2†}

¹Hanyang University

²Seoul University

Abstract

Video Action Detection (VAD) involves localizing and categorizing action instances in videos. Videos inherently contain various information sources, including audio, visual cues, and surrounding scene contexts. Effectively leveraging this multi-modal information for VAD is challenging, as the model must accurately focus on action-relevant cues. In this study, we introduce a novel multi-modal VAD architecture called the Joint Actor-centric Visual, Audio, Language Encoder (JoVALE). JoVALE is the first VAD method to integrate audio and visual features with scene descriptive context derived from large image captioning models. The core principle of JoVALE is the actor-centric aggregation of audio, visual, and scene descriptive contexts, where action-related cues from each modality are identified and adaptively combined. We propose a specialized module called the Actor-centric Multi-modal Fusion Network, designed to capture the joint interactions among actors and multi-modal contexts through Transformer architecture. Our evaluation conducted on three popular VAD benchmarks, AVA, UCF101-24, and JHMDB51-21, demonstrates that incorporating multi-modal information leads to significant performance gains. JoVALE achieves state-of-the-art performances. The code will be available at <https://github.com/taeiin/AAAI2025-JoVALE>.

Introduction

Video action detection (VAD) is a challenging task that aims to localize and classify human actions within video sequences. VAD generates bounding boxes with action scores for a keyframe by analyzing the sequential frames around the keyframe. This task differs from *Action Recognition* task, which classifies the action for a given video clip, and from *Temporal Action Detection* task, which identifies the intervals of particular actions within a video clip.

Humans rely on various sources of information to detect actions, including visual appearance, motion sequences, actor postures, and interactions with their environment. Numerous studies have demonstrated that leveraging multiple modalities can significantly enhance action recognition performance (Kazakos et al. 2019; Gao et al. 2020; Xiao et al. 2020; Nagrani et al. 2021). Audio, in particular, offers valu-

able information, providing both direct and indirect contextual cues for action recognition. For example, sounds directly linked to actions, like speech, gunshots, or music, can help identify corresponding actions. Additionally, environmental sounds can indirectly suggest relevant actions, such as the sound of waves indicating beach-related activities. Therefore, incorporating audio data alongside visual data can improve the performance and robustness of VAD. Several action recognition methods have successfully utilized both audio and visual data to enhance performance (Gao et al. 2020; Xiao et al. 2020; Nagrani et al. 2021).

While multi-modal information has proven effective for action recognition tasks, applying it to VAD is challenging. Action instances are dispersed across both temporal and spatial domains within a video. In addition, the contextual cues necessary for detecting these actions are scattered throughout the video as well. Thus, VAD models must selectively focus on the relevant information needed to detect each specific action instance. For example, the sound of a piano can assist in identifying a ‘playing piano’ action but may be irrelevant for detecting a ‘talking with others’ action within the same scene. In addition, effectively combining information from different modalities is crucial to optimizing VAD performance. The use of audio-visual information for VAD remains an underexplored area in the literature.

Another valuable source for VAD identified in this study is the prior general knowledge acquired through vision-language foundation models. Recently, Vision Language Pre-training (VLP) models have achieved significant success by utilizing vast amounts of multi-modal data from the web, public databases, and various corpora. These VLP models are capable of capturing complex relational structures between text and images, enabling them to generalize to various downstream tasks in a zero-shot or one-shot manner. Given their high-level understanding of images, the knowledge obtained through VLP can be leveraged to enhance VAD. In this study, we also explore a VAD approach that utilizes the comprehensive language context provided by VLP.

This paper introduces a novel multi-modal VAD approach referred to as the Joint Actor-centric Visual, Audio, Language Encoder (JoVALE). JoVALE is the first method to leverage audio and visual modalities alongside language context to localize and classify actions in videos. At the core of JoVALE is the actor-centric modeling of multi-modal

*These authors contributed equally.

†Corresponding author. Email: junwchoi@snu.ac.kr

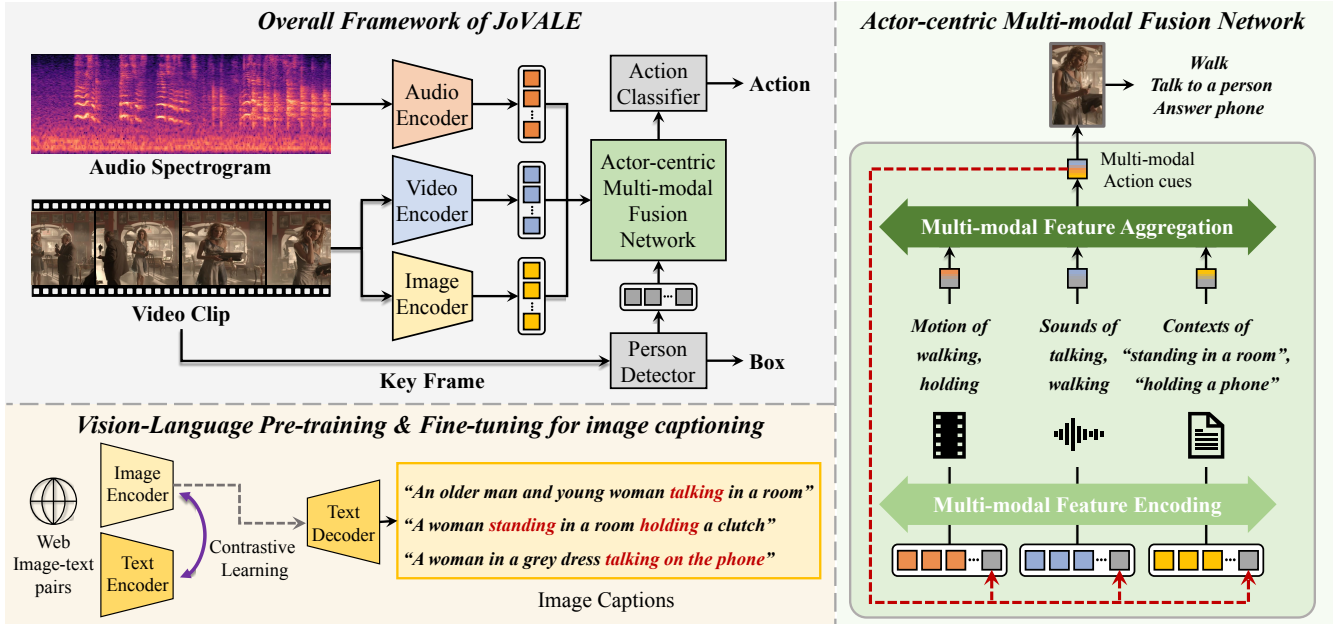


Figure 1: Overview of JoVALE: The proposed JoVALE generates audio, visual, and scene-descriptive features and integrates them using an Actor-centric Multi-modal Fusion Network (AMFN). (top-left) JoVALE leverages a VLP model fine-tuned on an image captioning task to generate scene-descriptive features. (bottom-left) AMFN encodes high-level interactions between multi-modal features through Multi-modal Feature Extraction and Multi-modal Feature Aggregation. (right)

contextual information.

The key concepts of JoVALE are illustrated in Fig. 1. JoVALE begins by generating densely sampled actor proposal features using a person detector. These actor proposal features are then processed by the Actor-centric Multi-modal Fusion Network (AMFN), which aggregates relevant contextual information from both audio and visual features. Furthermore, AMFN integrates scene-descriptive knowledge acquired from the VLP model, BLIP (Li et al. 2022a), to enhance the action representation.

To fully leverage multi-modal information for VAD, JoVALE effectively models the relationships among actors, temporal dynamics, and different modalities. Our AMFN framework successively captures their complex interactions by refining Action Embeddings across multiple Transformer layers. AMFN consists of Multi-modal Feature Encoding (MFE) and Multi-modal Feature Aggregation (MFA). The MFE module jointly encodes Action Embeddings and Multi-modal Context Embeddings within each modality. Temporal Bottleneck Features, a compact representation of the temporal changes across all actors, are used to make an encoding process efficient. Next, the MFA module aggregates the Action Embeddings from each modality in a weighted manner. These aggregated features are then fed into the subsequent Transformer layer.

We evaluated JoVALE on three popular VAD benchmarks: AVA (Gu et al. 2018), UCF101-24 (Soomro, Zamir, and Shah 2012), and JHMDB51-21 (Jhuang et al. 2013). By effectively combining audio, visual, and scene-descriptive context information, JoVALE significantly outperforms the

baseline on these benchmarks. On the highly complex and challenging AVA dataset, JoVALE records a mean Average Precision (mAP) of 40.1%, achieving a substantial improvement of 2.4% over the previous best method, EVAD (Chen et al. 2023).

Our contributions can be summarized as follows:

- We present a simple, yet effective multi-modal VAD architecture that utilizes the audio-visual information present in videos. Our main approach is Actor-Centric Feature Aggregation, which adaptively attends to the multi-modal context essential for detecting each action instance. There are only a few studies that have explored the use of audio-visual context for VAD.
- We are the first to introduce a VAD approach that incorporates general scene-descriptive knowledge inferred from a Vision Language Foundation model.
- We propose an efficient architecture that effectively models complex relationships among actors, temporal dynamics, and modalities. Our modeling approach differs from existing VAD methods, which typically combine semantic actor features or predicted scores from each modality in a straightforward manner.

Related Work

Video Action Detection

Various VAD methods have been proposed to date, which can be broadly categorized into two main approaches: end-to-end and two-stage methods. End-to-end methods predict

both the location of the action and the action class simultaneously within a single network. These methods often employ a query-based approach using Transformers (Vaswani et al. 2017). Notable examples of end-to-end VAD methods include VTr (Girdhar et al. 2019), TubeR (Zhao et al. 2022), STMixer (Wu et al. 2023), and EVAD (Chen et al. 2023). In contrast, two-stage VAD methods first utilize a pre-trained person detector to localize the actors and identify where the action occurs before classifying the actions. Examples of these methods include AIA (Tang et al. 2020) and ACAR (Pan et al. 2021). Recently, Vision Transformers (Tong et al. 2022; Wang et al. 2023a,b), pre-trained with Masked Autoencoders (MAE) (He et al. 2022), have shown outstanding performance in the context of two-stage VAD.

Multi-modal Video Action Detection

Early multi-modal VAD methods (Gkioxari and Malik 2015; Saha et al. 2016; Zhao and Snoek 2019) leveraged both RGB and optical flow to capture appearance and motion information. Another research direction focused on utilizing human skeletal structures through pose estimation models. For example, JMNRN (Shah et al. 2022) extracted individual joint features and captured inter-joint correlations. More recently, HIT (Faure, Chen, and Lai 2023) employed cross-attention mechanisms to capture interactions between key action-related components such as hands, objects, and poses.

While various video understanding methods that leverage both audio and visual information have been extensively studied (Gao et al. 2020; Xiao et al. 2020; Nagrani et al. 2021; Gong et al. 2022; Georgescu et al. 2023; Huang et al. 2024), the use of audio-visual context specifically for VAD has not been explored in depth. This task presents unique challenges, as the relevant audio-visual context for effective VAD may vary depending on the specific action instance being detected. This study aims to address this gap.

Method

Overview

The overall structure of JoVALE is illustrated in Fig. 1. Audio samples and sequence of image frames are provided to the model as input. Audio and visual backbone features are derived from these inputs, while scene-descriptive features are obtained from the BLIP image encoder. These features form the multi-modal contexts used for VAD.

JoVALE detects actions through the following steps. Based on the keyframe image, an off-the-shelf person detector generates K actor proposals along with their corresponding Region of Interest (RoI) features, referred to as Actor Proposal Features. The AMFN then attends to the action-related information within the separately encoded backbone features using a Transformer attention. As depicted in Fig.2, the AMFN comprises two modules: MFE and MFA. The AMFN jointly encodes the Action Embeddings $a_a^{(l)}$, $a_v^{(l)}$, and $a_s^{(l)}$ that correspond to audio, visual, and scene-descriptive embeddings, respectively. Note that l denotes the layer index. Each Action Embeddings is represented by a 3D tensor with actor, time, and channel dimensions. In the first layer, the Action Embeddings are all ini-

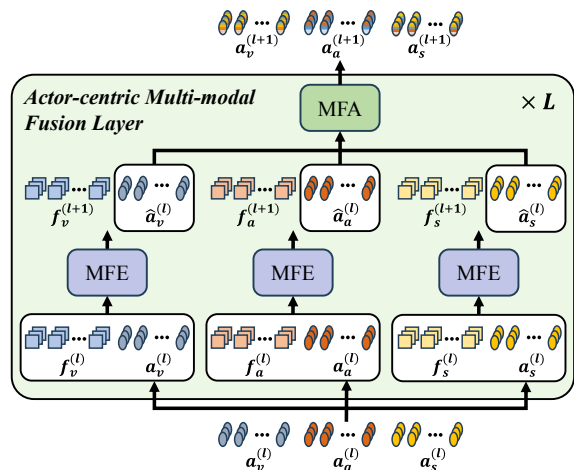


Figure 2: Structure of AMFN: Three independent MFEs encode the context features within each modality. Then, MFA combines Action Embeddings derived from each modality.

tialized with the Actor Proposal Features. For each modality, MFE module encodes the Action Embeddings $a_{mod}^{(l)}$ and Multi-modal Context Embeddings $f_{mod}^{(l)}$ jointly, where mod in $\mathcal{M} = \{a, v, s\}$. Self-Attention operation updates these embeddings into the Action Embeddings $\hat{a}_{mod}^{(l)}$ and the Multi-modal Context Embeddings $f_{mod}^{(l+1)}$. Using a gated fusion mechanism (Kim et al. 2018), the MFA module then performs a weighted combination of the three Action Embeddings, $\hat{a}_a^{(l)}$, $\hat{a}_v^{(l)}$, and $\hat{a}_s^{(l)}$, producing the combined Action Embeddings $a_a^{(l+1)}$, $a_v^{(l+1)}$, and $a_s^{(l+1)}$. These Action Embeddings are used for the next layer. This process is iterated L times, successively refining the Action Embeddings. The final Action Embeddings from the L -th layer are then fed into the classifier to predict action instances.

Generating Multi-modal Features

Visual Embeddings. We encode an input video clip using a video backbone network such as SlowFast (Feichtenhofer et al. 2019) and ViT (Dosovitskiy et al. 2020). This process generates spatio-temporal features $F_v \in \mathbb{R}^{T_v \times H \times W \times C}$, where T_v , H , W , and C represent temporal, spatial, and channel dimensions, respectively. These features are then reshaped into sequences of N_v feature vectors per time step, where $N_v = HW$. Subsequently, these vectors are linearly projected into visual embeddings $f_v \in \mathbb{R}^{T_v \times N_v \times D}$, where D denotes the embedding dimension.

Audio Embeddings. Following existing audio preprocessing techniques (Gong, Chung, and Glass 2021), we transform audio waveform samples into a log-mel-spectrogram in time and frequency bins. This spectrogram is fed into a convolution layer with kernel size $P \times P$ and stride S , then reshaped into sequences of N_a feature vectors. This process results in audio embeddings $f_a \in \mathbb{R}^{T_a \times N_a \times D}$.

Scene-Descriptive Embeddings. Scene-descriptive features are generated using the BLIP captioner (Li et al.

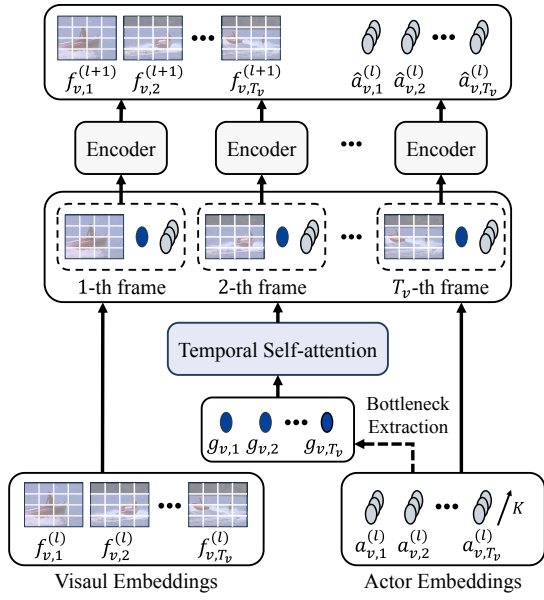


Figure 3: Structure of Multi-modal Feature Encoding. This illustration depicts the process for the visual modality. Identical structures are applied individually to other modalities.

2022a), a vision-language foundation model that is fine-tuned on an image captioning task. The BLIP captioner takes each image frame as input, encodes it with an image encoder, and produces a text description of the image through a text decoder. Since the output of the image encoder contains high-level semantic scene information that can be readily translated into the text, we can use it as scene-descriptive features. We first uniformly sample T_s image frames from a video clip. Then, we apply the image encoder of the BLIP captioner to each of T_s image frames. The resulting feature maps are then linearly projected into the scene-descriptive embeddings $f_s \in \mathbb{R}^{T_s \times N_s \times D}$.

Actor-centric Multi-modal Fusion Network

AMFN updates Action Embeddings $a_a^{(l)}$, $a_v^{(l)}$, and $a_s^{(l)}$ by applying MFE and MFA in an iterative fashion.

Multi-modal Feature Encoding. The structure of MFE is shown in Fig. 3. The MFE performs the following operation

$$\hat{a}_{mod}^{(l)}, f_{mod}^{(l+1)} = \text{MFE} \left(a_{mod}^{(l)}, f_{mod}^{(l)} \right). \quad (1)$$

Applying self-attention to the combination of $a_{mod}^{(l)}$ and $f_{mod}^{(l)}$ may lead to high computational complexity when the number of actors and temporal resolution are large. To reduce this complexity, we generate Temporal Bottleneck Features that summarize the temporal embeddings across actors at each time step. By taking $a_{mod}^{(l)} \in \mathbb{R}^{K \times T_{mod} \times D}$ as an input, MFE computes the Temporal Bottleneck Features, $b_{mod}^{(l)} \in \mathbb{R}^{T_{mod} \times D}$ from

$$b_{mod}^{(l)} = \text{SA}(\text{Pool}(a_{mod}^{(l)})), \quad (2)$$

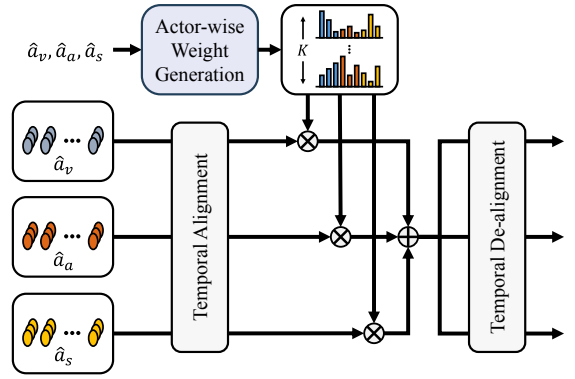


Figure 4: Structure of Multi-modal Feature Aggregation.

where Pool refers to the average pooling over the actor dimension and SA denotes the multi-head self-attention. Note that this SA operation encodes the Action Embeddings in the time domain. Finally, the Temporal Bottleneck Features are merged to the Multi-modal Context Embeddings $f_{mod,t}^{(l)}$ and the Action Embeddings $a_{mod,t}^{(l)}$. Then, MFE encodes the relation among actors and contexts for each time step

$$\hat{a}_{mod,t}^{(l)}, f_{mod,t}^{(l+1)} = \text{Encoder}(a_{mod,t}^{(l)}, f_{mod,t}^{(l)}, b_{mod,t}^{(l)}), \quad (3)$$

where $t \in [1, T_{mod}]$, Encoder consists of a SA, two normalization layers, and an FFN. Finally, the updated Action Embeddings $\hat{a}_a^{(l)}$, $\hat{a}_v^{(l)}$, and $\hat{a}_s^{(l)}$ are delivered to MFA module.

Multi-modal Feature Aggregation. The structure of MFA is depicted in Fig. 4. The MFA operates as follows

$$a_v^{(l+1)}, a_a^{(l+1)}, a_s^{(l+1)} = \text{MFA}(\hat{a}_v^{(l)}, \hat{a}_a^{(l)}, \hat{a}_s^{(l)}). \quad (4)$$

MFA starts with Temporal Alignment, which aligns time sampling between the Action Embeddings $\hat{a}_v^{(l)}$, $\hat{a}_a^{(l)}$, and $\hat{a}_s^{(l)}$. Following (Cooper 2019), the Action Embeddings of size T_{mod} in time dimension are resized to those of the fixed size T_c . Then, MFA adaptively integrates query features $\hat{a}_v^{(l)}$, $\hat{a}_a^{(l)}$, $\hat{a}_s^{(l)}$ for each actor using an adaptive gating mechanism. Specifically, MFA concatenates Action Embeddings and applies average pooling over the time dimension

$$a_p^{(l)} = \text{Pool}([\hat{a}_v^{(l)} \parallel \hat{a}_a^{(l)} \parallel \hat{a}_s^{(l)}]), \quad (5)$$

where \parallel denotes channel-wise concatenation. We obtain the combining weights by passing the pooled features through a bottleneck MLP followed by a sigmoid function

$$[w_v^{(l)} \parallel w_a^{(l)} \parallel w_s^{(l)}] = \sigma(\text{MLP}(a_p^{(l)})), \quad (6)$$

where MLP consists of two fully connected layers with an activation function and $\sigma(\cdot)$ denotes sigmoid function. Note that different combining weights are obtained for different actors. The resulting cross-modal weights are used to recalibrate actor embeddings as

$$a_{fuse}^{(l)} = \frac{1}{|\mathcal{M}|} \sum_{m \in \mathcal{M}} w_m^{(l)} \otimes \hat{a}_m^{(l)} \quad (7)$$

$$a_{mod}^{(l+1)} = a_{fuse}^{(l)} + w_{mod}^{(l)} \otimes \hat{a}_{mod}^{(l)}, \quad (8)$$

Model	Input	Backbone	Pre-train	Val mAP
Models with 3D-CNN backbones				
WOO (Chen et al. 2021)	32×2	SF-R101	K600	28.3
SlowFast (Feichtenhofer et al. 2019)	32×2	SF-R101	K600	29.0
AIA (Tang et al. 2020)	32×2	SF-R101	K700	32.3
ACAR (Pan et al. 2021)	32×2	SF-R101	K700	33.3
TubeR (Zhao et al. 2022)	32×2	CSN-152	K400	33.6
HIT (Faure, Chen, and Lai 2023)	32×2	SF-R101	K700	32.6
STMixer (Wu et al. 2023)	32×2	SF-R101	K700	30.9
JoVALE	32×2	SF-R101	K700	35.5
Models with ViT backbones				
VideoMAE (Tong et al. 2022)	16×4	ViT-B	K400	31.8
MViTv2 (Li et al. 2022b)	32×3	MViTv2-B	K700	32.3
MeMViT (Wu et al. 2022)	32×3	MViTv2-B	K700	34.4
MVD (Wang et al. 2023b)	16×4	ViT-B	K400	34.2
STMixer (Wu et al. 2023)	16×4	ViT-B [†]	K710	36.1
EVAD (Chen et al. 2023)	16×4	ViT-B [†]	K710	37.7
JoVALE	16×4	ViT-B [†]	K710	40.1

Table 1: Performance comparison on the AVA 2.2 dataset. ViT-B marked with [†] is initialized with pre-trained weights from VideoMAE v2 (Wang et al. 2023a).

where \otimes denotes the element-wise multiplication.

Then, the Action Embeddings $a_a^{(l+1)}, a_v^{(l+1)}, a_s^{(l+1)}$ are converted back to those of their own temporal sampling. After L layers, the classification head is applied to $a_{fuse}^{(L)}$ to predict action scores $c \in \mathbb{R}^{K \times N_{cls}}$, where N_{cls} denotes the number of target classes in the dataset. These scores, along with the corresponding actor bounding boxes $b \in \mathbb{R}^{K \times 4}$, form a set of action instances (b, c) .

Experiments

Datasets & Metrics

We evaluate JoVALE, on three standard VAD datasets: AVA (Gu et al. 2018), UCF101-24 (Soomro, Zamir, and Shah 2012), and JHMDB51-21 (Jhuang et al. 2013). AVA consists of 299 15-minute movie clips, with 235 for training and 64 for validation. We evaluate our approach on 60 action classes in AVA v2.2. UCF101-24, a subset of UCF101, contains 24 sport action classes with 3,207 instances, and our method is evaluated on the first split. JHMDB51-21, a subset of JHMDB51, includes 928 trimmed video clips spanning 21 action classes. We report the average performance across the three standard splits of the dataset. The evaluation metric is frame-level mAP at an Intersection over Union (IoU) threshold of 0.5 for all datasets.

Implementation Details

In this section, we describe the implementation details of our proposed JoVALE. The implementation specifics and detailed architectural descriptions of various JoVALE models are provided in the *Supplementary Material*.

Generating Multi-modal Features. Visual feature extraction was conducted using one of the following backbones: SlowFast-R50 pre-trained on Kinetics-400 (Kay et al. 2017), SlowFast-R101 pre-trained on Kinetics-700 (Carreira et al. 2019), or ViT-B with pre-trained weights from VideoMAE v2.

Audio preprocessing followed the approach in (Gong, Chung, and Glass 2021), where log-mel-spectrograms were extracted from raw audio waveforms. The waveforms, sampled at 16kHz, were converted into 128 Mel-frequency bands using a 25ms Hamming window with a 10ms stride, resulting in spectrograms of dimension $100t \times 128$.

Scene-descriptive features were extracted using the ViT-B BLIP captioner, which was pre-trained on 14 million images from COCO, Visual Genome (Krishna et al. 2017), and web datasets (Changpinyo et al. 2021; Ordonez, Kulkarni, and Berg 2011), and subsequently fine-tuned on the COCO Caption dataset.

Initializing Action Embeddings. We employed a Faster R-CNN (Ren et al. 2015) with a ResNeXt-101-FPN (Lin et al. 2017; Xie et al. 2017) as a person detector. The detector was pre-trained on ImageNet (Russakovsky et al. 2015) and COCO human keypoint images (Lin et al. 2014) and fine-tuned on each target VAD dataset. The top K actor features were extracted from the penultimate layer based on human confidence scores.

Training. The pre-trained person detector and image captioner were kept frozen during both training and inference. The entire model was trained using sigmoid focal loss for action classification. The AdamW optimizer was employed with a weight decay of $1e-4$. Initial learning rates were set to $1e-5$ for the video backbone and $1e-4$ for the other networks,

Model	Input	Backbone	Pre-train	UCF	JHMDB
AVA	20 × 1	I3D	K400	76.3	73.3
AIA	32 × 1	C2D	K400	78.8	-
ACRN	20 × 1	S3D-G	K400	-	77.9
CARN	32 × 2	I3D-R50	K400	-	79.2
YOWO	16 × 1	3D-RX-101	K400	75.7	80.4
WOO	32 × 2	SF-R101	K600	-	80.5
TubeR	32 × 2	CSN-152	K400	83.2	-
ACAR*	32 × 1	SF-R50	K400	84.3	-
HIT*	32 × 2	SF-R50	K700	84.8	83.8
STMixer	32 × 2	SF-R101	K700	83.7	86.7
JoVALE	32 × 2	SF-R101	K700	84.9	91.0

Table 2: Performance comparison on UCF101-24 and JHMDB51-21. The models marked with * employ YOWO (Köpükü, Wei, and Rigoll 2019) as a person detector.

with a tenfold reduction applied at the 7th epoch. Training was conducted for 8 epochs with a batch size of 16, utilizing four NVIDIA GeForce RTX 3090 GPUs.

Main Results

Performance Comparison. We compare JoVALE against existing VAD methods across three widely used datasets. As shown in Table 1, JoVALE achieves superior performance on the AVA dataset, outperforming existing methods across both 3D-CNN and ViT backbone based methods. With a 3D-CNN backbone, JoVALE surpasses the previous best method, STMixer (Wu et al. 2023), by 1.9 mAP. Using a ViT backbone, JoVALE sets a new state-of-the-art on AVA, outperforming EVAD (Chen et al. 2023) by 2.4 mAP.

Table 2 presents the results on the UCF101-24 and JHMDB51-21 datasets, where we employed SF-101 as the visual backbone. Since over 80% of the video clips in these datasets lack audio, JoVALE utilizes only visual and scene-descriptive features as input. Even without audio, JoVALE achieves the best performance, with mAP scores of 84.9 on UCF101-24 and 91.0 on JHMDB51-21.

Ablation Study

Our ablation studies were conducted on AVA v2.2 using the SlowFast-R50 configuration. For computational complexity analysis, we used 256×256 square input frames. Unless stated otherwise, all other settings were consistent with the main experiments. Detailed model configurations used in these ablations are provided in the *Supplementary Material*.

Effect of Multi-modalities. In Table 3, we evaluate the impact of various combinations of modalities in JoVALE. Among single modalities, visual information achieves the highest performance, indicating the importance of motion cues. In comparison, using audio information alone results in a lower performance, suggesting its limitations when used independently. When visual and scene descriptive embeddings are fused, the mAP increases to 32.7. This improvement emphasizes the role of linguistic context in enriching the visual context and enhancing semantic understanding. The integration of all three modalities peak performance

with an mAP of 34.0, suggests that the complementary interaction across modalities is decisive in maximizing accuracy. These experimental results provide empirical evidence supporting the effectiveness of multi-modalities in VAD.

Method	Modality			mAP
	Video	Audio	Scene-desc.	
Uni-modal	✓			28.0
		✓		11.5
			✓	26.9
Multi-modal	✓	✓		28.6
	✓		✓	32.7
		✓	✓	27.8
	✓	✓	✓	34.0

Table 3: Impact of various combinations of modalities.

Effect of Multi-modal Fusion Strategies. Next, we compare our JoVALE model with commonly used fusion strategies in multi-modal VAD. In this experiment, we excluded audio features because the RoI feature extraction used in previous approaches is not applicable to audio data. We report the computational cost of the entire model, excluding the person detector. As shown in Table 4, relation modeling on RoI actor features (Faure, Chen, and Lai 2023) significantly improves performance compared to RoI feature fusion (Gkioxari and Malik 2015) with an increase of 0.7 mAP. To further explore global inter-modal dependencies, we employed a Transformer encoder that processes the unified multi-modal context as input. While this approach significantly improved performance, it also led to a substantial increase in computational complexity. While this highlights the effectiveness of comprehensive relation modeling in multi-modal VAD, it also substantially increases computational complexity. In contrast, JoVALE achieved the highest mAP of 32.7 while maintaining computational efficiency. These results demonstrate the superiority of our multi-modal fusion strategy.

Methods	GFLOPs	mAP
RoI feature fusion	320.5	29.1
RoI relation modeling	320.7	30.4
Global relation modeling	370.3	32.1
JoVALE	342.1	32.7

Table 4: Effect of Multi-modal fusion strategies.

Effect of MFE. We explored various MFE architectures for effectively extracting spatio-temporal features. Table 5 presents the performance and computational costs of AMFN with different MFE configurations. As a baseline, we employed a Transformer that encodes spatio-temporal features jointly within a single encoder, achieving 33.8 mAP but with high computational complexity. Based on ViViT (Arnab et al. 2021), TimeSFormer (Bertasius, Wang, and Torresani

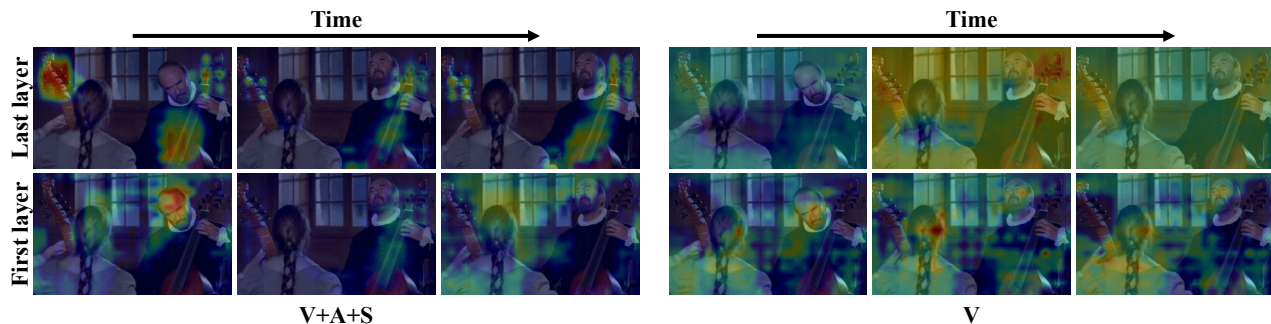


Figure 5: Visualization of activation maps. The left side shows heatmaps for the JoVALE model utilizing audio, visual, and scene-descriptive features, while the right side shows heatmaps for the JoVALE model using only visual features.

Multi-modal Feature Encoding	GFLOPs	mAP
Transformer	41.7	33.8
ViViT	23.0	30.6
TimeSformer	31.2	33.1
XCLIP	24.4	32.4
MFE	25.4	34.0

Table 5: Comparison between diverse multi-modal feature encoding approaches.

2021), and XCLIP (Ni et al. 2022), we implemented various temporal modeling techniques to enhance efficiency. While these methods constrain the information flow between temporal and spatial dimensions to enhance computational efficiency, this comes at the cost of reduced performance. In contrast, our MFE leverages bottleneck features derived from actor features, facilitating the exchange of crucial actor-centric information. By focusing on actor-relevant information, our method effectively balances the trade-off between model complexity and performance, achieving superior performance with 34.0 mAP and maintaining computational efficiency at 25.4 GFLOPs.

Effect of MFA. Table 6 presents an ablation study analyzing the key components of MFA. The key components of MFA consist of an iterative structure that progressively fuses multi-modal features and a gated fusion that adaptively combines multi-modal features from individual MFEs. We first establish a baseline method that simply fuses the predicted action scores from individual MFEs. To evaluate the effectiveness of the iterative structure, we then assessed a structure that repeatedly applies MFE followed by average pooling. Despite the simple fusion method, this structure shows a significant performance improvement of 2.5 mAP. This gain highlights the benefit of progressively refining multi-modal features. Applying the gated fusion approach to the baseline method achieves a substantial performance gain of 3.7 mAP, underscoring the effectiveness of adaptively fusing multi-modal information for each actor. Finally, combining the iterative structure and gated fusion yields a remarkable 4.6 mAP improvement over the baseline, demonstrating the effectiveness of our proposed MFA.

Methods	Iterative structure	Gated fusion	mAP
Baseline			29.4
	✓		31.9
MFA		✓	33.1
	✓	✓	34.0

Table 6: Component analysis of Multi-modal Feature Aggregation.

Qualitative Results

Fig. 5 compares the activation maps of multi-modal JoVALE, which incorporates visual, audio, and scene-descriptive features, with those of JoVALE using only visual features. In both the first layer (bottom row) and the final layer (top row), the multi-modal JoVALE demonstrates a stronger focus on musical instruments, particularly evident in the final layer. These results suggest that the multi-modal JoVALE effectively uses audio information to identify instrument sounds and focus on relevant areas. The iterative structure of JoVALE appears to leverage inter-modal relationships, progressively improving instrument recognition through audio cues. This visualization shows that JoVALE can gain insights from audio data that visual data alone might miss, and it gradually integrates multi-modal information by exploiting inter-modal dependencies. In summary, this analysis demonstrates that JoVALE’s multi-modal approach offers a more comprehensive understanding of scenes compared to uni-modal methods.

Conclusion

In this paper, we introduced JoVALE, a novel multi-modal architecture for video action detection that effectively integrates audio, visual, and scene-descriptive language information. Our method, centered on actor-centric modeling of multi-modal contextual information, overcomes the limitations of single-modality approaches and generates rich action representations. JoVALE’s key innovations include the Actor-centric Multi-modal Fusion Network (AMFN), enabling efficient modeling of complex relationships among

actors, temporal dynamics, and different modalities. Extensive experiments on challenging VAD benchmarks demonstrate that JoVALE achieves state-of-the-art performance, significantly surpassing existing methods.

References

- Arnab, A.; Deghani, M.; Heigold, G.; Sun, C.; Lučić, M.; and Schmid, C. 2021. Vivit: A video vision transformer. In *Proceedings of the IEEE/CVF international conference on computer vision*, 6836–6846.
- Bertasius, G.; Wang, H.; and Torresani, L. 2021. Is space-time attention all you need for video understanding? In *ICML*, volume 2, 4.
- Carreira, J.; Noland, E.; Hillier, C.; and Zisserman, A. 2019. A short note on the kinetics-700 human action dataset. *arXiv preprint arXiv:1907.06987*.
- Changpinyo, S.; Sharma, P.; Ding, N.; and Soricut, R. 2021. Conceptual 12m: Pushing web-scale image-text pre-training to recognize long-tail visual concepts. In *Proceedings of the IEEE/CVF conference on computer vision and pattern recognition*, 3558–3568.
- Chen, L.; Tong, Z.; Song, Y.; Wu, G.; and Wang, L. 2023. Efficient video action detection with token dropout and context refinement. In *Proceedings of the IEEE/CVF International Conference on Computer Vision*, 10388–10399.
- Chen, S.; Sun, P.; Xie, E.; Ge, C.; Wu, J.; Ma, L.; Shen, J.; and Luo, P. 2021. Watch only once: An end-to-end video action detection framework. In *Proceedings of the IEEE/CVF International Conference on Computer Vision*, 8178–8187.
- Cooper, A. 2019. Hear me out: hearing each other for the first time: the implications of cochlear implant activation. *Missouri medicine*, 116(6): 469.
- Dosovitskiy, A.; Beyer, L.; Kolesnikov, A.; Weissenborn, D.; Zhai, X.; Unterthiner, T.; Deghani, M.; Minderer, M.; Heigold, G.; Gelly, S.; et al. 2020. An image is worth 16x16 words: Transformers for image recognition at scale. *arXiv preprint arXiv:2010.11929*.
- Faure, G. J.; Chen, M.-H.; and Lai, S.-H. 2023. Holistic interaction transformer network for action detection. In *Proceedings of the IEEE/CVF Winter Conference on Applications of Computer Vision*, 3340–3350.
- Feichtenhofer, C.; Fan, H.; Malik, J.; and He, K. 2019. Slow-fast networks for video recognition. In *Proceedings of the IEEE/CVF International Conference on Computer Vision*, 6202–6211.
- Gao, R.; Oh, T.-H.; Grauman, K.; and Torresani, L. 2020. Listen to look: Action recognition by previewing audio. In *Proceedings of the IEEE/CVF conference on computer vision and pattern recognition*, 10457–10467.
- Georgescu, M.-I.; Fonseca, E.; Ionescu, R. T.; Lucic, M.; Schmid, C.; and Arnab, A. 2023. Audiovisual masked autoencoders. In *Proceedings of the IEEE/CVF International Conference on Computer Vision*, 16144–16154.
- Girdhar, R.; Carreira, J.; Doersch, C.; and Zisserman, A. 2019. Video action transformer network. In *Proceedings of the IEEE/CVF Conference on Computer Vision and Pattern Recognition*, 244–253.
- Gkioxari, G.; and Malik, J. 2015. Finding action tubes. In *Proceedings of the IEEE conference on computer vision and pattern recognition*, 759–768.
- Gong, Y.; Chung, Y.-A.; and Glass, J. 2021. Ast: Audio spectrogram transformer. *arXiv preprint arXiv:2104.01778*.
- Gong, Y.; Rouditchenko, A.; Liu, A. H.; Harwath, D.; Karlinsky, L.; Kuehne, H.; and Glass, J. 2022. Contrastive audio-visual masked autoencoder. *arXiv preprint arXiv:2210.07839*.
- Gu, C.; Sun, C.; Ross, D. A.; Vondrick, C.; Pantofaru, C.; Li, Y.; Vijayanarasimhan, S.; Toderici, G.; Ricco, S.; Sukthankar, R.; et al. 2018. Ava: A video dataset of spatio-temporally localized atomic visual actions. In *Proceedings of the IEEE Conference on Computer Vision and Pattern Recognition*, 6047–6056.
- He, K.; Chen, X.; Xie, S.; Li, Y.; Dollár, P.; and Girshick, R. 2022. Masked autoencoders are scalable vision learners. In *Proceedings of the IEEE/CVF conference on computer vision and pattern recognition*, 16000–16009.
- Huang, P.-Y.; Sharma, V.; Xu, H.; Ryali, C.; Li, Y.; Li, S.-W.; Ghosh, G.; Malik, J.; Feichtenhofer, C.; et al. 2024. Mavil: Masked audio-video learners. *Advances in Neural Information Processing Systems*, 36.
- Jhuang, H.; Gall, J.; Zuffi, S.; Schmid, C.; and Black, M. J. 2013. Towards understanding action recognition. In *Proceedings of the IEEE International Conference on Computer Vision*, 3192–3199.
- Kay, W.; Carreira, J.; Simonyan, K.; Zhang, B.; Hillier, C.; Vijayanarasimhan, S.; Viola, F.; Green, T.; Back, T.; Natsev, P.; et al. 2017. The kinetics human action video dataset. *arXiv preprint arXiv:1705.06950*.
- Kazakos, E.; Nagrani, A.; Zisserman, A.; and Damen, D. 2019. Epic-fusion: Audio-visual temporal binding for ego-centric action recognition. In *Proceedings of the IEEE/CVF international conference on computer vision*, 5492–5501.
- Kim, J.; Koh, J.; Kim, Y.; Choi, J.; Hwang, Y.; and Choi, J. W. 2018. Robust deep multi-modal learning based on gated information fusion network. In *Asian Conference on Computer Vision*, 90–106. Springer.
- Köpüklü, O.; Wei, X.; and Rigoll, G. 2019. You only watch once: A unified cnn architecture for real-time spatiotemporal action localization. *arXiv preprint arXiv:1911.06644*.
- Krishna, R.; Zhu, Y.; Groth, O.; Johnson, J.; Hata, K.; Kravitz, J.; Chen, S.; Kalantidis, Y.; Li, L.-J.; Shamma, D. A.; et al. 2017. Visual genome: Connecting language and vision using crowdsourced dense image annotations. *International journal of computer vision*, 123: 32–73.
- Li, J.; Li, D.; Xiong, C.; and Hoi, S. 2022a. Blip: Bootstrapping language-image pre-training for unified vision-language understanding and generation. In *International Conference on Machine Learning*, 12888–12900. PMLR.
- Li, Y.; Wu, C.-Y.; Fan, H.; Mangalam, K.; Xiong, B.; Malik, J.; and Feichtenhofer, C. 2022b. Mvitv2: Improved multi-scale vision transformers for classification and detection. In *Proceedings of the IEEE/CVF conference on computer vision and pattern recognition*, 4804–4814.

- Lin, T.-Y.; Dollár, P.; Girshick, R.; He, K.; Hariharan, B.; and Belongie, S. 2017. Feature pyramid networks for object detection. In *Proceedings of the IEEE Conference on Computer Vision and Pattern Recognition*, 2117–2125.
- Lin, T.-Y.; Maire, M.; Belongie, S.; Hays, J.; Perona, P.; Ramanan, D.; Dollár, P.; and Zitnick, C. L. 2014. Microsoft coco: Common objects in context. In *Computer Vision—ECCV 2014: 13th European Conference, Zurich, Switzerland, September 6–12, 2014, Proceedings, Part V 13*, 740–755. Springer.
- Nagrani, A.; Yang, S.; Arnab, A.; Jansen, A.; Schmid, C.; and Sun, C. 2021. Attention bottlenecks for multimodal fusion. *Advances in neural information processing systems*, 34: 14200–14213.
- Ni, B.; Peng, H.; Chen, M.; Zhang, S.; Meng, G.; Fu, J.; Xiang, S.; and Ling, H. 2022. Expanding language-image pre-trained models for general video recognition. In *European Conference on Computer Vision*, 1–18. Springer.
- Ordonez, V.; Kulkarni, G.; and Berg, T. 2011. Im2text: Describing images using 1 million captioned photographs. *Advances in neural information processing systems*, 24.
- Pan, J.; Chen, S.; Shou, M. Z.; Liu, Y.; Shao, J.; and Li, H. 2021. Actor-context-actor relation network for spatio-temporal action localization. In *Proceedings of the IEEE/CVF Conference on Computer Vision and Pattern Recognition*, 464–474.
- Ren, S.; He, K.; Girshick, R.; and Sun, J. 2015. Faster r-cnn: Towards real-time object detection with region proposal networks. *Advances in Neural Information Processing Systems*, 28.
- Russakovsky, O.; Deng, J.; Su, H.; Krause, J.; Satheesh, S.; Ma, S.; Huang, Z.; Karpathy, A.; Khosla, A.; Bernstein, M.; et al. 2015. Imagenet large scale visual recognition challenge. *International journal of computer vision*, 115: 211–252.
- Saha, S.; Singh, G.; Sapienza, M.; Torr, P. H.; and Cuzzolin, F. 2016. Deep learning for detecting multiple space-time action tubes in videos. *arXiv preprint arXiv:1608.01529*.
- Shah, A.; Mishra, S.; Bansal, A.; Chen, J.-C.; Chellappa, R.; and Shrivastava, A. 2022. Pose and joint-aware action recognition. In *Proceedings of the IEEE/CVF Winter Conference on Applications of Computer Vision*, 3850–3860.
- Soomro, K.; Zamir, A. R.; and Shah, M. 2012. UCF101: A dataset of 101 human actions classes from videos in the wild. *arXiv preprint arXiv:1212.0402*.
- Tang, J.; Xia, J.; Mu, X.; Pang, B.; and Lu, C. 2020. Asynchronous interaction aggregation for action detection. In *Computer Vision—ECCV 2020: 16th European Conference, Glasgow, UK, August 23–28, 2020, Proceedings, Part XV 16*, 71–87. Springer.
- Tong, Z.; Song, Y.; Wang, J.; and Wang, L. 2022. Videomae: Masked autoencoders are data-efficient learners for self-supervised video pre-training. *Advances in neural information processing systems*, 35: 10078–10093.
- Vaswani, A.; Shazeer, N.; Parmar, N.; Uszkoreit, J.; Jones, L.; Gomez, A. N.; Kaiser, Ł.; and Polosukhin, I. 2017. Attention is all you need. *Advances in neural information processing systems*, 30.
- Wang, L.; Huang, B.; Zhao, Z.; Tong, Z.; He, Y.; Wang, Y.; Wang, Y.; and Qiao, Y. 2023a. Videomae v2: Scaling video masked autoencoders with dual masking. In *Proceedings of the IEEE/CVF Conference on Computer Vision and Pattern Recognition*, 14549–14560.
- Wang, R.; Chen, D.; Wu, Z.; Chen, Y.; Dai, X.; Liu, M.; Yuan, L.; and Jiang, Y.-G. 2023b. Masked video distillation: Rethinking masked feature modeling for self-supervised video representation learning. In *Proceedings of the IEEE/CVF Conference on Computer Vision and Pattern Recognition*, 6312–6322.
- Wu, C.-Y.; Li, Y.; Mangalam, K.; Fan, H.; Xiong, B.; Malik, J.; and Feichtenhofer, C. 2022. Memvit: Memory-augmented multiscale vision transformer for efficient long-term video recognition. In *Proceedings of the IEEE/CVF Conference on Computer Vision and Pattern Recognition*, 13587–13597.
- Wu, T.; Cao, M.; Gao, Z.; Wu, G.; and Wang, L. 2023. Stmixer: A one-stage sparse action detector. In *Proceedings of the IEEE/CVF Conference on Computer Vision and Pattern Recognition*, 14720–14729.
- Xiao, F.; Lee, Y. J.; Grauman, K.; Malik, J.; and Feichtenhofer, C. 2020. Audiovisual slowfast networks for video recognition. *arXiv preprint arXiv:2001.08740*.
- Xie, S.; Girshick, R.; Dollár, P.; Tu, Z.; and He, K. 2017. Aggregated residual transformations for deep neural networks. In *Proceedings of the IEEE Conference on Computer Vision and Pattern Recognition*, 1492–1500.
- Zhao, J.; and Snoek, C. G. 2019. Dance with flow: Two-in-one stream action detection. In *Proceedings of the IEEE/CVF conference on computer vision and pattern recognition*, 9935–9944.
- Zhao, J.; Zhang, Y.; Li, X.; Chen, H.; Shuai, B.; Xu, M.; Liu, C.; Kundu, K.; Xiong, Y.; Modolo, D.; et al. 2022. Tuber: Tubelet transformer for video action detection. In *Proceedings of the IEEE/CVF Conference on Computer Vision and Pattern Recognition*, 13598–13607.